Composites Part B 219 (2021) 108932

Contents lists available at ScienceDirect

Composites Part B

journal homepage: www.elsevier.com/locate/compositesb

Transfer printed laser induced graphene strain gauges for embedded sensing in fiberglass composites

LoriAnne Groo [a], Jalal Nasser [a], Daniel J. Inman [a], Henry A. Sodano [a,b,c,*]

[a] Department of Aerospace Engineering, University of Michigan, Ann Arbor, MI, 48109, United States
[b] Department of Macromolecular Science and Engineering, University of Michigan, Ann Arbor, MI, 48109, United States
[c] Department of Materials Science and Engineering, University of Michigan, Ann Arbor, MI, 48109, United States

ARTICLE INFO

Keywords:
Laser induced graphene
Multifunctional composites
Strain sensor
Fiber-reinforced composites
In-situ sensing

ABSTRACT

The continuous monitoring of strain in fiber-reinforced composites while in service typically requires bonding a network of sensors to the surface of the composite structure. To eliminate such needs, and to reduce bulk and limit additional weight, this work utilizes the transfer printing of laser induced graphene (LIG) strain gauges onto the surface of commercial fiberglass prepreg for the in situ self-sensing of strain. The resultant embedded strain sensor is entirely integrated within the final composite material, therefore reducing weight and eliminating limitations due to external bonding compared to current alternatives. Additionally, the simple printing process used here allows for the customization of the size and sensing requirements for various applications. The LIG strain sensor is shown to be capable of tracking monotonic cyclic strain as shown during tensile loading and unloading of the host composite, while also proving capable of tracking the dynamic motion of the composite which is characterized via frequency response and sinusoidal base excitation. The LIG strain gauge in this work can thus be used for tracking either quasi-static or dynamic variations in strain for the determination of the deformation experienced by the material, as well as the frequency content of the material for structural health monitoring purposes.

1. Introduction

In-situ structural health monitoring (SHM) of fiber-reinforced composites has drawn significant research attention as it has the potential to meet multiple industrial needs such as improved safety and decreased maintenance costs. Initial investigation into SHM methods utilized external sensors to meet these needs, however, a desire to increase application by reducing limitations placed by external systems has led to the investigation and development of various smart and multifunctional materials. Some of the most common current in-situ monitoring methods include acoustic emission testing (AET) [1,2], optical fibers [3,4], and resistance-based sensing [5,6]. Among these methods, resistance-based sensing holds an advantage for multiple reasons including the ability to sense both strain and damage as well as the potential to sense changes in state both in-situ and ex-situ. Although optical fibers are also capable of sensing both strain and damage with composites, the method requires that the sensors are aligned in the same direction as the reinforcing fibers to avoid compromising the load-bearing capabilities of the composite [7]. For in-situ and non-invasive sensing of strain, commercial piezoresistive materials are commonly used, as the measurable change in resistance from these materials correlates to the local strain of the structure to which they are attached. Commercial strain gauges are typically comprised of a flexible polymer with a thin metal wire in a serpentine pattern. Commonly, these piezoresistive-based strain sensors use metallic materials or semiconductors such as silicon (N or P type) due to their high gauge factor, which is reliable for widespread use in dynamic loading applications. The change in resistance allows highly sensitive strain monitoring in-situ; however, commercial strain gauges require external bonding to the structure or material under investigation. This imposes limitations on the physical characteristics of the surface such as texture, smoothness, and curvature, in addition to limiting the monitored area to the surface ply of the composite. In addition, embedding the strain gauge within the composite to measure the strain of each ply individually increases the risk of delamination due to the addition of the sensor within the inter-ply area, further weakening the failure-prone interlaminar region of the composite.

To overcome the current restrictions of commercial strain gauges,

* Corresponding author. Department of Aerospace Engineering, University of Michigan, Ann Arbor, MI, 48109, United States.
E-mail address: hsodano@umich.edu (H.A. Sodano).

https://doi.org/10.1016/j.compositesb.2021.108932
Received 1 June 2020; Received in revised form 9 April 2021; Accepted 18 April 2021
Available online 30 April 2021
1359-8368/

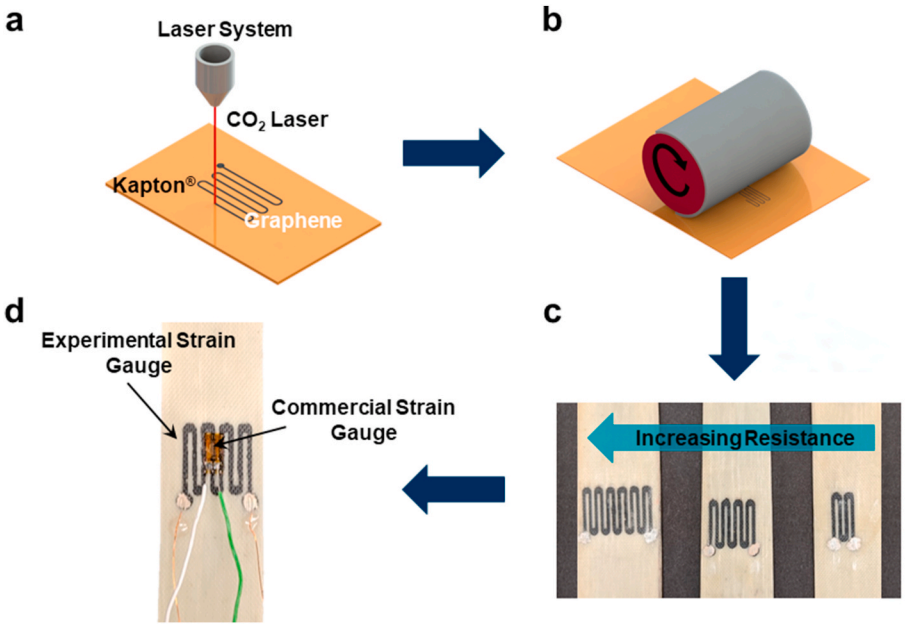

Fig. 1. Schematic of the LIG (a) printing and (b) transfer processes. (c) Image of transfer printed strain gauges with varying resistance. (d) Image of completed sample with LIG and commercial strain gauges.

research has turned to the investigation of alternative piezoresistive nano- or micro-scale materials such as metallic particles, graphene oxide or nanoplatelets, carbon nanotubes (CNTs), or some combination of these materials [5,6,8–14]. Three main approaches have been used to incorporate these nanomaterials within fiberglass-reinforced composites: fabricating stand-alone material components comprised solely of the nanomaterials, fabricating sensing materials comprised of nanomaterials held together by various polymer matrices, or distributing the nanomaterials within the composite either along the fiber reinforcement or in the uncured matrix. The first approach investigating standalone sensing materials has been investigated by multiple researchers resulting in buckypaper sensors fabricated from CNT networks [15–18] and individual yarns comprised of CNTs [19], both of which proved the capability of effectively sensing strain. However, the gauge factor and sensitivity of CNT-based strain gauges are dependent on the orientation of the CNTs, which is difficult to control due to agglomerations formed as a result of van der Waals forces [20]. Additionally, in each case, discrete embedding within fiber reinforced composites is needed since individual sensing components are used, thus limiting the sensing area and further complicating the fabrication processes. Using the second approach, further research has utilized CNTs distributed within various polymer matrices [21–24], spray coating CNTs onto polyimide films to create individual strain sensors [25], and graphene nanoplatelet coated spandex yarns [26] either embedded within the composite or attached to the composite surface for localized strain sensing. Each of these methodologies was again shown to be sensitive to the strain of the composite structure under investigation, however, a uniform dispersion of the CNTs within a polymer network plays a crucial role in the final strain sensitivity. Furthermore, uniform CNT dispersion is difficult to achieve due to their tendency to agglomerate [27,28]. Additionally, the resultant individual strain gauges, although effective in measuring strain, still require external bonding or embedding within fiber-reinforced composites for in-situ sensing. Similarly, using the third approach, several researchers have shown that the inclusion of piezoresistive nanomaterials within the fiber-reinforced composites can be used for SHM via the coating of fiberglass with graphene nanoplatelets [14], and the distribution of CNTs in the uncured matrix of the composite [29,30]. However, it was not possible to achieve a complete or an even distribution of the graphene nanoplatelets on the surface of the fiberglass [14]. In addition, even distribution of the CNTs is complicated to spatially control due to filtering that can result from resin flow through a fiber preform in combination with the previously discussed restrictions prohibiting widespread application, such difficulty in orienting CNTs and agglomerations due to van der Waals forces. Therefore, an alternative approach is required to expand the use of multifunctional materials for the in-situ strain monitoring of fiberglass-reinforced composites.

Laser induced graphene (LIG) is a promising alternative to the more common CNT-based strain sensors due to the simplicity of the methodology and the design flexibility [31]. The simple LIG process uses a common CO_2 infrared laser in ambient environmental conditions to irradiate polyimides, converting sp^3-carbon atoms to sp^2-carbon atoms, to generate a porous graphitic surface with piezoresistive properties. Therefore, the polyimide is used as the precursor for the graphitic surface, and no external graphene source is required, resulting in a simple, scalable, and automatable process. Since its initial discovery, the piezoresistive behavior of LIG has been investigated for several applications including biomedical applications [32,33], composite strain sensing [34–36], and flexible strain sensors [37,38]. For example, Luo et al. generated LIG strain gauges on polyimide films which were then glued to the surface of fiberglass-reinforced composites and used to sense deformation of the host composite [35]. Although the LIG was shown to be sensitive to material strain in this and other applications, the need for external bonding to the composite structure has not yet been eliminated and remains an issue due to the strict requirements it places on the state of the surface such as surface roughness, curvature, and compatibility with adhesive materials. As an alternative method, Wang et al. generated a free-standing LIG-based buckypaper which was then embedded between prepreg layers and used to monitor composite cure and strain [34]. However, the mechanical properties of the resultant composite were not investigated, and the gauge factor of the buckypaper-prepreg composite was not reported. Thus, an alternative method allowing for strategic placement and pre-determined size and sensing capability without affecting the host material properties or requiring external bonding for a variety of continuous fiber reinforced surfaces is still needed. Here, we demonstrate a tailorable non-invasive strain gauge for fiber reinforced composites that fills a gap in the field of scalable SHM and structural sensing.

This work explores the use of LIG for the transfer printing of LIG-

based strain gauges and their integration within fiberglass-reinforced composites. The strain gauges are customized for the size of the monitored material and are then directly printed onto polyimide tape using a commercial CO_2 laser cutter. The LIG sensors are then subsequently transferred to the surface of commercial fiberglass prepreg, before subjecting them to cyclic monotonic loading and dynamic testing to confirm their ability to sense both quasi-static and dynamic strain. The commercial prepreg used in this work required no prior treatment or modification, and no alignment procedures were necessary for the LIG strain gauges. Instead, once the strain gauges are transfer printed to the surface of the prepreg, resistance measurements are made using wires attached directly to the surface of the composite in combination with a Wheatstone bridge. Thus, this work enables embedded sensing of fiberglass composites by incorporating a tailorable sensor within the structural composite itself. This is especially beneficial in the case of geometrically complex or curved structures or in extreme environments where externally bonded sensors lack feasibility or robustness. The result is therefore a scalable, multifunctional, self-sensing material.

2. Materials and methods

2.1. LIG and composite fabrication

LIG was produced using a commercial laser cutter (Epilog Zing 16 universal laser machine) with a CO_2 40 W infrared laser. The graphitic microstructure was printed into serpentine patterns (between 0.4 and 0.8 inches in width and 1 inch in height) onto 2 mil (0.0254 mm) Kapton® tape sheets as shown in Fig. 1a. For effective transfer, the rastered laser beam was pulsed at 14% power such that it fired 400 times per inch yielding a print at 400 dots per inch (DPI). It should be noted that variation in the power, speed, and DPI can be used to adjust the density and resistivity of the resulting LIG patterns [35]. The graphene layer used in this work has a fuzzy texture which is transferrable to the tacky surface of a Solvay E773 prepreg with S-glass fibers (CYCOM® S-Glass/E773). This results in the microstructure and the printed serpentine pattern being largely maintained during transfer [36]. In order to further improve the transfer, the prepreg was heated to 80 °C on a hotplate for approximately 1 min, which increases the tackiness of the prepreg such that the LIG adheres to the surface. The LIG pattern was then transferred to the prepreg using a constant pressure rolling process which is illustrated in Fig. 1b. The effective length of the printed LIG was varied by controlling the length of the serpentine pattern printed (Fig. 1c) in order to establish a trend between the resistance of the strain gauge and the resulting gauge factor during quasi-static testing. Following the transfer of the LIG strain gauge to the prepreg, two additional plies of neat unidirectional prepreg were added to complete the layup for mechanical testing. The ply with the transferred strain gauge was placed on top in the layup to enable direct strain measurements from the composite. The layup was then cured at 121 °C (250 °F) for 2 h under vacuum at 100 psi (689 kPa) in a hot press. It can be noted that previous work has confirmed that pre-heating the prepreg to 80 °C and adding the LIG has no effect on the sample cure, and that the addition of the LIG results in no measurable changes in weight or thickness in contrast to externally bonded sensors [36]. Following the composite cure, samples were cut to a width of one inch and length of four inches, and wire leads (33-gauge copper wire) were directly attached to the conductive LIG strain gauge ends using a combination of silver paint and epoxy. Finally, a commercial strain gauge was attached to the surface of the completed composite specimen to provide reference strain measurements. An image of the final composite sample is shown in Fig. 1d where it can be observed that the tailorable LIG sensing element is entirely embedded within the composite structure.

2.2. Quasi-static tensile testing

Following the completion of the sample fabrication, the samples were subjected to quasi-static tensile testing. Reference measurements were obtained using a commercial strain gauge (VISHAY® micro-measurements & SR-4 general purpose strain gauge, 120 ± 0.3% Ω, 2.075 ± 0.5% gauge factor) that was mounted to the surface of the sample (Fig. 1d) and coupled with a Wheatstone bridge and millivolt amplifier (Omega™ model MN1400-4). The constant voltage input for the Wheatstone bridge used with the commercial strain gauge was provided by a Hewlett Packard model 6217A DC power supply. The resistance of the LIG strain gauge was monitored using a second Wheatstone bridge, in combination with a Transducer Techniques TMO-2 signal conditioner. A schematic of the measurement method is shown in Fig. 2. An Instron model 5982 with a 100 kN load cell was used for tensile testing, and the samples were subjected to quasi-static cyclic loading 20 times with the load ranging from zero to 1200 N, which was previously determined to be well below the load at which the composite displays indications of damage. Prior to testing, current was applied to the bridge for several minutes to allow the LIG sample to thermally equilibrate. Following completion of the test, the gauge factor of the LIG strain gauges was identified using a linear fit of the resistance change to the true strain measured by the commercial strain gauge for each cycle. The average gauge factor over the 20 quasi-static cycles was then used to calculate the strain as measured by the LIG strain gauge for each composite sample.

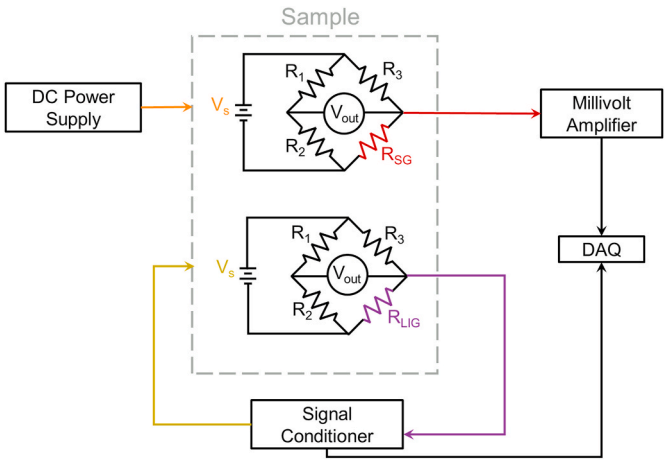

Fig. 2. Schematic of measurement methods for one test specimen.

2.3. Dynamic strain sensing

In addition to sensing quasi-static strain, the ability to measure dynamic strain was also evaluated. To establish their dynamic capabilities, the fiberglass beams with LIG strain gauges were mounted in a cantilever configuration and excited with an impulse using a PCB model 086C03 impact hammer measured through a PCB 482A16 signal conditioner. The frequency response of the sample, using resistance measurements from the LIG strain gauge and the impulse measurement from the impact hammer, was then calculated to determine the natural frequency of the sample. To examine the ability of the samples to track a sine wave at a random frequency away from resonance, the samples were also excited at their base with a sine wave using a Keysight 33500B series waveform generator and Labworks Inc. pa-119 power amplifier in combination with an LDS electromagnetic shaker system. The base acceleration of the sample was measured during excitation using a PCB 352C22 accelerometer in combination with the PCB 482A16 signal conditioner. During each measurement, the resistance of the sample was again monitored using a Wheatstone bridge in combination with a Transducer Techniques TMO-2 signal conditioner.

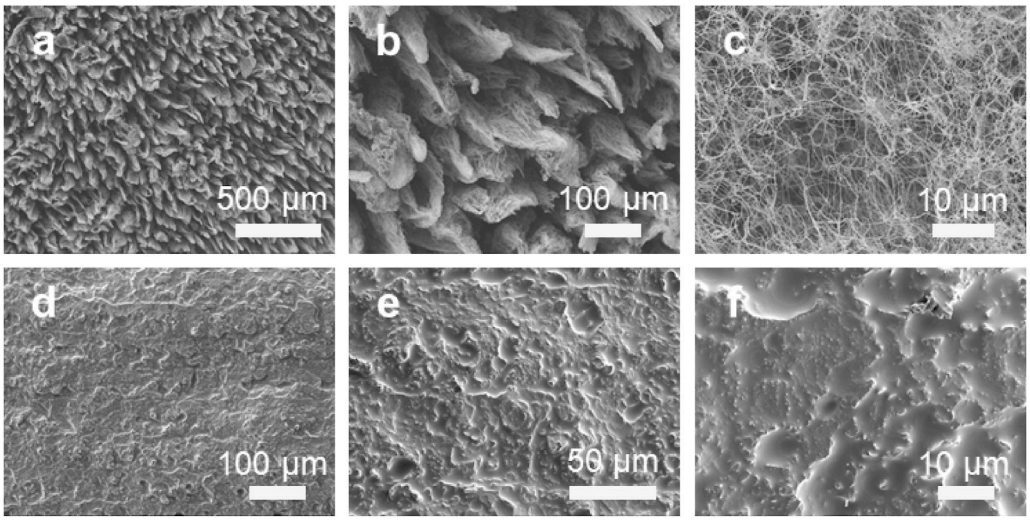

Fig. 3. Images of LIG taken using a scanning electron microscope (SEM) (a–c) before transfer and (d–f) after transfer to fiberglass prepreg and subsequent curing.

3. Results and discussion

3.1. LIG characterization

Using a commercial CO_2 laser, LIG was printed in a serpentine pattern, rather than a solid rectangular block, in order to increase the distance between the two measurement points while minimizing the amount of space occupied by the LIG strain gauge. This design thus takes advantage of a longer conductive pathway to increase the change in resistance due to the piezoresistance of the LIG. However, it can be noted that the laser pathway can be altered to fit specific design requirements, such as the area of interest. To characterize the resultant LIG on the surface of the polyimide tape and the surface of the fiberglass prepreg following the transfer process, the surfaces were imaged using a scanning electron microscope (SEM) (JSM-7800F). From Fig. 3a through Fig. 3c, the fuzzy LIG microstructure on the surface of the polyimide is comprised of pillars of entangled individual graphene fibers. This microstructure is preserved during the transfer from the polyimide tape to the prepreg surface with only a slight longitudinal compression [36], before being completely embedded in the matrix once the composite is cured as can be seen in Fig. 3d through Fig. 3f. As the prepreg is heated during cure, the matrix softens and infuses the porous LIG. The final product is thus a composite with a piezoresistive strain sensor that is fully integrated within the matrix in a manner that does not compromise the structural integrity of the composite [36]. It should be noted that the LIG retains low electrical impedance values following transfer, as the microstructure is not significantly altered during the process. However, using the current method, a small fraction of the LIG remains exposed at the surface of the composite which enables the straight-forward attachment of wire leads directly onto the surface of the sample without requiring the removal of matrix from the surface. The transfer printing process is more fully discussed and characterized elsewhere [36]. If additional protection for the printed strain gauges was required for future applications, the strain gauge plies could be placed at a different position in the stack sequence, or a protective coating could be added to the surface of the composite to fully encapsulate the LIG. The resulting printed strain gauges were approximately 0.4–0.8 inches in width and an inch in height for tensile samples which had an approximate 1 inch width, however the size of the strain gauge could be varied for design purposes. Thus, the resulting dimensions are flexible depending on the end application with the main limitation being some dimensional accuracy due to the resolution of the commercial laser cutter used. Additionally, by varying the effective length of the printed strain gauge, the electrical impedance between the two contact points can be controlled during the first step of the transfer printing process. Using this methodology, a range of initial impedance values were tested to evaluate the effect of the impedance on the gauge factor of the LIG strain gauge. It is also worthwhile to note that the transfer printing process provides several benefits over alternative sensors. Since the LIG strain gauges are embedded within the matrix of the prepreg, the

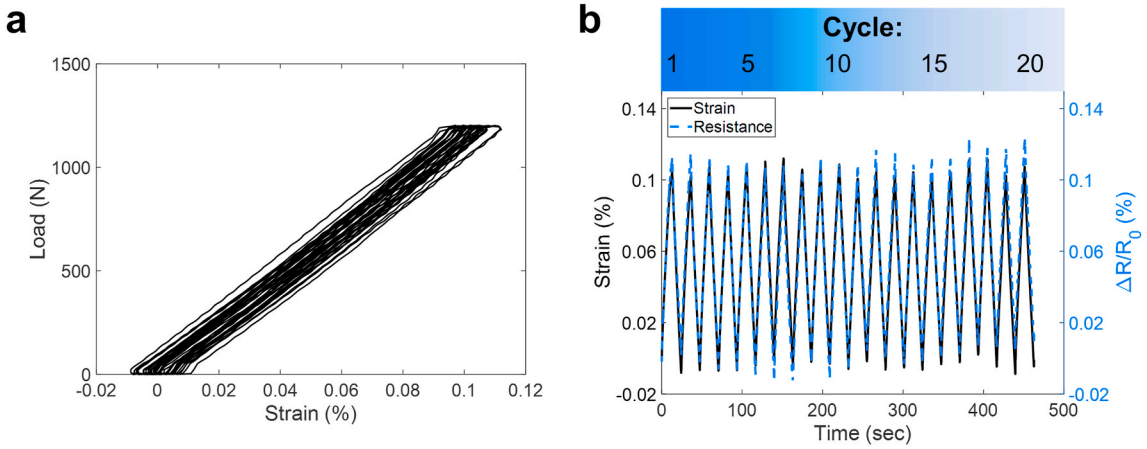

Fig. 4. (a) Load versus strain for one strain gauge sample. (b) Percent strain and percent change in resistance versus time for quasi-static cyclic loading.

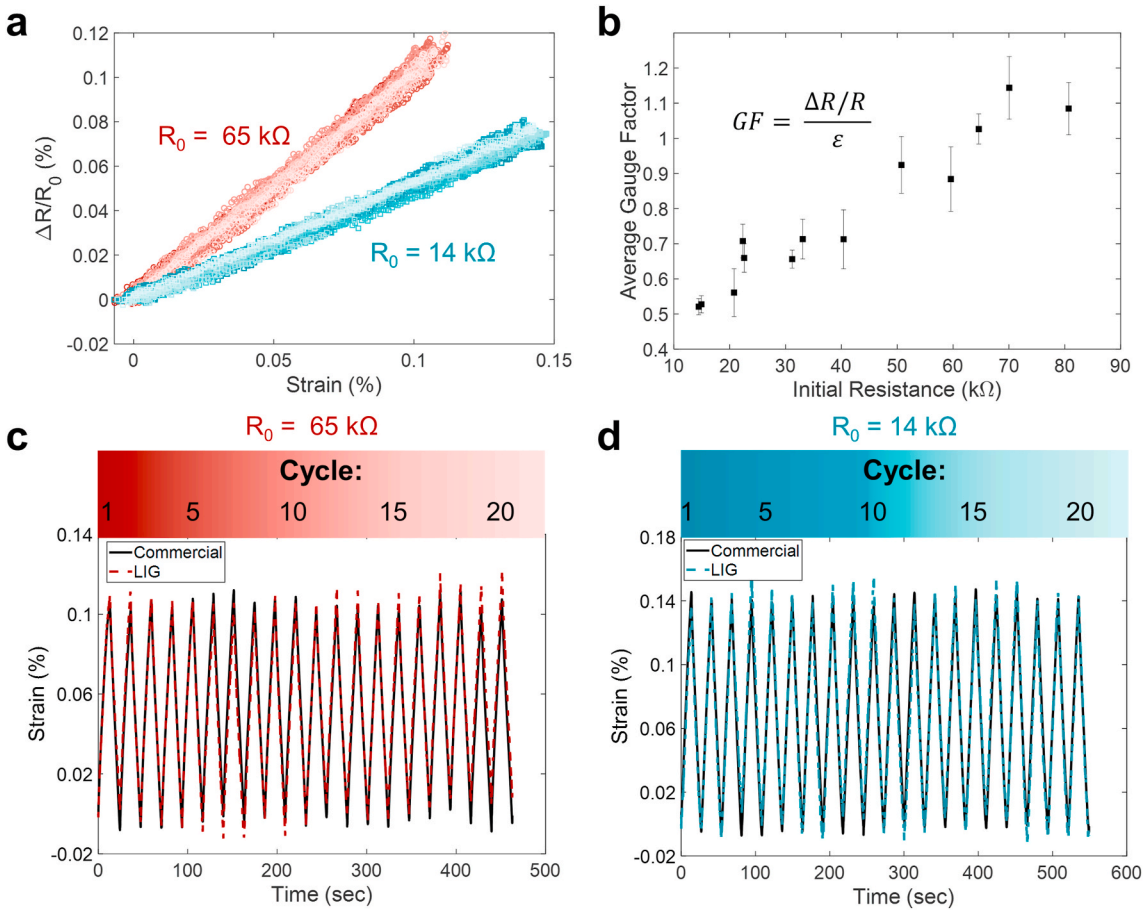

Fig. 5. (a) Percent change in resistance versus strain for increasing load over 20 cycles for two samples. (b) Gauge factor versus initial resistance. (c) Commercial strain and LIG strain versus time for high resistance sample. (d) Commercial strain and LIG strain versus time for low resistance sample.

methods used can be directly applied to alternative prepregs containing woven or chopped fibers rather than unidirectional fiber reinforcement. Additionally, the strain gauge can be oriented in any direction relative to the fiber reinforcement, and can be used for strain sensing in geometrically complex or curved structures where externally bonded sensors are difficult or impossible to attach. Furthermore, since the design of the strain gauge is tailorable, the electrodes can be designed such that the external wires can be located in a preferential position for the required application.

3.2. Strain sensing during tensile testing

To evaluate the response of the LIG strain gauge during both loading and unloading, corresponding to increasing and decreasing strain, the samples were cycled between zero and 1200 N which was determined to be well below the threshold at which the composite experienced significant damage. The applied load versus strain measured by the commercial strain gauge for one sample is shown for reference in Fig. 4a. The experimental results from the commercial strain gauge versus time in comparison to the percent change in resistance of the LIG during the same test are shown in Fig. 4b. From this representative sample it can be seen that the LIG shows very little additional noise or signal distortion in comparison to the commercial strain gauge, and instead smoothly transitions from loading to unloading and vice versa. Furthermore, the samples exhibited minimal error and noise between the LIG strain and the commercial strain regardless of the effective size or final gauge factor of the LIG strain gauge. It can be noted that the LIG results also display no residual change in resistance, and instead show a full recovery within the range tested here. At a microscale, the LIG senses strain by taking advantage of its inherent piezoresistance; as a load is applied and the LIG is positively strained, small microcracks or gaps form within the microstructure of the LIG, resulting in a decrease in conductive contacts and an increase in electrical impedance [37,38]. As both load and strain are decreased, these microcracks and the conductive pathways are repaired, thus resulting in a repeatable effect [37,38]. Since little to no mechanical damage or plastic deformation was caused in the host fiberglass structure, no permanent separation within the LIG strain gauge is observed to occur, and the measurements show a full recovery as the load is removed. However, it is worthwhile to note that the embedded nature of the LIG inherently couples it with the composite structure. Therefore, damage to the composite would result in damage to the sensor and lead to changes in the response of the LIG. This response to damage is more fully discussed elsewhere [36].

The strain measured by the LIG was calculated based on the averaged ratio between the normalized change in resistance of the LIG (ΔR/R) and the commercial strain (ε), known as the gauge factor (GF), calculated from the loading portion of each cycle (Fig. 5b). To accurately calculate a representative gauge factor for each sample, a linear fit between the percent change in resistance and the percent change in strain (determined by the commercial strain gauge) was used for each leg of increasing strain over 20 cycles, and the results were averaged. For reference, the percent change in resistance versus the percent strain for two samples, one with relatively high initial resistance (65 kΩ) and one with relatively low initial resistance (14 kΩ), are shown in Fig. 5a. The resulting LIG-based strain of the same two samples are compared to the strain from commercial strain gauges in Fig. 5c and d. From these representative samples, although the overall error was variant based on each sample, the commercial and LIG strain show very close agreement

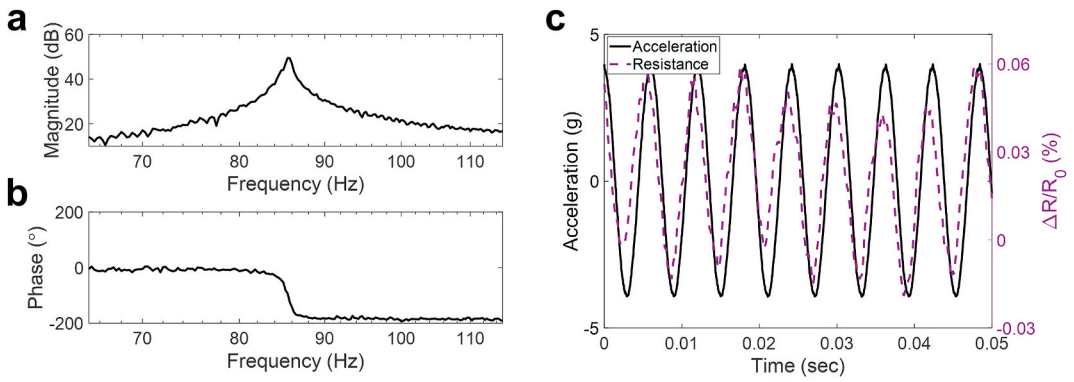

Fig. 6. (a) Magnitude and (b) phase of the frequency response of the sample resistance to an impulse. (c) Base acceleration and measured resistance of the strain gauge during sine wave excitation.

across most of the applied strain. While the majority of the cyclic loading exhibited negligible error, the points at which the sample transitions from an unloaded to a loaded state and vice versa result in the largest error values. This is anticipated to be due to a slight delay in response as the LIG begins to stretch or compress, resulting in a decrease or increase in carbon-carbon contacts, respectively. In particular, some LIG and commercial strain gauges showed significant misalignment at strain values very close to 0%; however, it should be noted that some of the error between the commercial strain gauge and the LIG measurements can also be attributed to the error of the commercial strain gauge itself. To further characterize the LIG-based strain gauges, the gauge factor of the LIG in comparison to its initial resistance was investigated by examining the trend over several samples with varying initial resistance values. From Fig. 5b, the average gauge factors of the samples show an increasing trend with initial resistance, which indicates that the gauge factor is tailorable by controlling the initial resistance of the LIG-based strain gauge during the laser printing process. Although the gauge factor of the LIG is below that of the commercial strain gauge, the LIG strain gauge adds negligible weight and no bulk to the structure, while also eliminating the need for external adhesion and surface requirements such as limitations on surface roughness or curvature. Therefore, the LIG strain gauge shows a fully integrated alternative to the commercial strain gauge, removing the need for surface bonding and relatively extensive processing and preparation required by the commercial strain gauge.

3.3. Dynamic strain testing

The dynamic response of the strain gauge was evaluated using two approaches: the determination of the natural frequency using an impact hammer, and the measurement of the dynamic response of a cantilevered beam subjected to a sine wave base excitation. Fig. 6a and Fig. 6b show the magnitude and phase of the frequency response of the sample resistance from an impulse hammer excitation, respectively. The natural frequency of the sample is clearly detectable from the strong peak in the magnitude which coincides with a 180° phase shift. These results indicate that the resistance measurements from the LIG strain gauge can be used to track the frequency content of the beam for the purpose of material and damage characterization or for the tracking of vibrations experienced by a structure in service. In addition, the sample was excited with a sine wave at a randomly chosen frequency of 165 Hz, which was away from resonance, and the change of resistance of the LIG strain gauge was again measured using a Wheatstone bridge and signal conditioner. The response of the LIG strain gauge is found to be a sine wave at the same frequency as that of the excitation, as shown in Fig. 6c. Therefore, the strain gauge is capable of tracking dynamic displacement locally, however it may be noted that a larger strain gauge or a system of printed strain gauges to be used in the case of a larger structure. Although this is a similar requirement to more common strain gauge materials, the addition of multiple LIG strain gauges to a composite will result in negligible additional weight and is not limited by surface requirements or size constraints as the LIG is integrated within the material component itself.

4. Conclusions

This work establishes the effective use of transfer printed LIG strain gauges for both quasi-static and dynamic embedded sensing in fiberglass-reinforced composites. The strain gauge size and approximate gauge factor are controlled through a commercial laser printing system that directly prints the strain gauges onto polyimide tape. The strain gauge is then transfer printed to commercial fiberglass, leading to the complete embedding of the strain gauge within the polymer matrix of the fiber-reinforced composite structure, providing a robust strain sensing functionality which avoids the need for complicated processing or orientation of the graphitic sensing material prior to application. The resulting gauge factors of the tested multifunctional samples range from 0.5 to 1.3, and the value was determined to be controllable by increasing or decreasing the effective length of the strain gauge. The response was also shown to be repeatable with no response distortion and little observable lag between the commercial and LIG strain responses. Furthermore, the dynamic results of the LIG strain gauges conclusively indicate that the LIG can also be used to monitor the frequency content of dynamic loading which is promising for future SHM applications. Therefore, the result of this work is the creation of a fully integrated strain gauge within a fiberglass composite with tailorable size, location, and gauge factor, which is capable of sensing both quasi-static and dynamic strain in-situ.

Author statement

LoriAnne Groo – conceptualization, investigation, writing – original draft, Jalal Nasser – conceptualization, investigation, writing – review and editing, Daniel J. Inman – project administration, methodology, writing – review and editing, funding acquisition, Henry A. Sodano – conceptualization, project administration, methodology, funding acquisition, supervision, writing – review and editing.

Declaration of competing interest

The authors declare that they have no known competing financial interests or personal relationships that could have appeared to influence the work reported in this paper.

Acknowledgements

This work was supported by the National Science Foundation Graduate Research Fellowship Program [grant number DGE 1256260]; National Science Foundation [grant numbers CMMI-1762369, EFRI-1935216]; and the Air Force Office of Scientific Research [contract number FA9550-16-1-0087].

References

[1] Huguet S, Godin N, Gaertner R, Salmon L, Villard D. Use of acoustic emission to identify damage modes in glass fibre reinforced polyester. Compos Sci Technol 2002;62(10):1433–44.
[2] Barré S, Benzeggagh ML. On the use of acoustic emission to investigate damage mechanisms in glass-fibre-reinforced polypropylene. Compos Sci Technol 1994;52(3):369–76.
[3] Kister G, Ralph B, Fernando GF. Damage detection in glass fibre-reinforced plastic composites using self-sensing E-glass fibres. Smart Mater Struct 2004;13(5):1166.
[4] Kuang K, Cantwell W. Use of conventional optical fibers and fiber Bragg gratings for damage detection in advanced composite structures: a review. Appl Mech Rev 2003;56(5):493–513.
[5] Böger L, Wichmann MH, Meyer LO, Schulte K. Load and health monitoring in glass fibre reinforced composites with an electrically conductive nanocomposite epoxy matrix. Compos Sci Technol 2008;68(7–8):1886–94.
[6] Gao S-l, Zhuang R-C, Zhang J, Liu J-W, Mäder E. Glass fibers with carbon nanotube networks as multifunctional sensors. Adv Funct Mater 2010;20(12):1885–93.
[7] Shivakumar K, Emmanwori L. Mechanics of failure of composite laminates with an embedded fiber optic sensor. J Compos Mater 2004;38(8):669–80.
[8] Thostenson ET, Chou T-W. Carbon nanotube networks: sensing of distributed strain and damage for life prediction and self healing. Adv Mater 2006;18(21):2837–41.
[9] Deng H, Lin L, Ji M, Zhang S, Yang M, Fu Q. Progress on the morphological control of conductive network in conductive polymer composites and the use as electroactive multifunctional materials. Prog Polym Sci 2014;39(4):627–55.
[10] Mahmood H, Vanzetti L, Bersani M, Pegoretti A. Mechanical properties and strain monitoring of glass-epoxy composites with graphene-coated fibers. Compos Appl Sci Manuf 2018;107:112–23.
[11] Muto N, Arai Y, Shin SG, Matsubara H, Yanagida H, Sugita M, et al. Hybrid composites with self-diagnosing function for preventing fatal fracture. Compos Sci Technol 2001;61(6):875–83.
[12] Lin L, Deng H, Gao X, Zhang S, Bilotti E, Peijs T, et al. Modified resistivity–strain behavior through the incorporation of metallic particles in conductive polymer composite fibers containing carbon nanotubes. Polym Int 2013;62(1):134–40.
[13] Eswaraiah V, Balasubramaniam K, Ramaprabhu S. Functionalized graphene reinforced thermoplastic nanocomposites as strain sensors in structural health monitoring. J Mater Chem 2011;21(34):12626–8.
[14] Moriche R, Jiménez-Suárez A, Sánchez M, Prolongo S, Ureña A. Graphene nanoplatelets coated glass fibre fabrics as strain sensors. Compos Sci Technol 2017;146:59–64.
[15] Lu S, Chen D, Wang X, Xiong X, Ma K, Zhang L, et al. Monitoring the manufacturing process of glass fiber reinforced composites with carbon nanotube buckypaper sensor. Polym Test 2016;52:79–84.
[16] Dharap P, Li Z, Nagarajaiah S, Barrera E. Nanotube film based on single-wall carbon nanotubes for strain sensing. Nanotechnology 2004;15(3):379.
[17] Luo S, Liu T. Structure–property–processing relationships of single-wall carbon nanotube thin film piezoresistive sensors. Carbon 2013;59:315–24.
[18] Wang X, Lu S, Ma K, Xiong X, Zhang H, Xu M. Tensile strain sensing of buckypaper and buckypaper composites. Mater Des 2015;88:414–9.
[19] Lekawa-Raus A, Koziol KK, Windle AH. Piezoresistive effect in carbon nanotube fibers. ACS Nano 2014;8(11):11214–24.
[20] Parmar K, Mahmoodi M, Park C, Park SS. Effect of CNT alignment on the strain sensing capability of carbon nanotube composites. Smart Mater Struct 2013;22(7):075006.
[21] Kang I, Schulz MJ, Kim JH, Shanov V, Shi D. A carbon nanotube strain sensor for structural health monitoring. Smart Mater Struct 2006;15(3):737–48.
[22] Loh KJ, Kim J, Lynch JP, Kam NWS, Kotov NA. Multifunctional layer-by-layer carbon nanotube–polyelectrolyte thin films for strain and corrosion sensing. Smart Mater Struct 2007;16(2):429.
[23] Knite M, Tupureina V, Fuith A, Zavickis J, Teteris V. Polyisoprene—multi-wall carbon nanotube composites for sensing strain. Mater Sci Eng C 2007;27(5–8):1125–8.
[24] Zhang W, Suhr J, Koratkar N. Carbon nanotube/polycarbonate composites as multifunctional strain sensors. J Nanosci Nanotechnol 2006;6(4):960–4.
[25] Lee D, Hong HP, Lee CJ, Park CW, Min NK. Microfabrication and characterization of spray-coated single-wall carbon nanotube film strain gauges. Nanotechnology 2011;22(45):455301.
[26] Montazerian H, Rashidi A, Dalili A, Najjaran H, Milani AS, Hoorfar M. Graphene-coated spandex sensors embedded into silicone sheath for composites health monitoring and wearable applications. Small 2019;15(17):1804991.
[27] Tehrani M, Boroujeni A, Hartman T, Haugh T, Case S, Al-Haik M. Mechanical characterization and impact damage assessment of a woven carbon fiber reinforced carbon nanotube–epoxy composite. Compos Sci Technol 2013;75:42–8.
[28] Gojny FH, Wichmann MHG, Köpke U, Fiedler B, Schulte K. Carbon nanotube-reinforced epoxy-composites: enhanced stiffness and fracture toughness at low nanotube content. Compos Sci Technol 2004;64(15):2363–71.
[29] Gao L, Thostenson ET, Zhang Z, Chou TW. Sensing of damage mechanisms in fiber-reinforced composites under cyclic loading using carbon nanotubes. Adv Funct Mater 2009;19(1):123–30.
[30] Gao L, Thostenson ET, Zhang Z, Byun J-H, Chou T-W. Damage monitoring in fiber-reinforced composites under fatigue loading using carbon nanotube networks. Phil Mag 2010;90(31–32):4085–99.
[31] Lin J, Peng Z, Liu Y, Ruiz-Zepeda F, Ye R, Samuel EL, et al. Laser-induced porous graphene films from commercial polymers. Nat Commun 2014;5:5714.
[32] Tao L-Q, Tian H, Liu Y, Ju Z-Y, Pang Y, Chen Y-Q, et al. An intelligent artificial throat with sound-sensing ability based on laser induced graphene. Nat Commun 2017;8:14579.
[33] Luong DX, Yang K, Yoon J, Singh SP, Wang T, Arnusch CJ, et al. Laser-induced graphene composites as multifunctional surfaces. ACS Nano 2019;13(2):2579–86.
[34] Wang Y, Wang Y, Zhang P, Liu F, Luo S. Laser-induced freestanding graphene papers: a new route of scalable fabrication with tunable morphologies and properties for multifunctional devices and structures. Small 2018;14(36):1802350.
[35] Luo S, Hoang PT, Liu T. Direct laser writing for creating porous graphitic structures and their use for flexible and highly sensitive sensor and sensor arrays. Carbon 2016;96:522–31.
[36] Groo L, Nasser J, Zhang L, Steinke K, Inman D, Sodano H. Laser induced graphene in fiberglass-reinforced composites for strain and damage sensing. Compos Sci Technol 2020:108367.
[37] Rahimi R, Ochoa M, Yu W, Ziaie B. Highly stretchable and sensitive unidirectional strain sensor via laser carbonization. ACS Appl Mater Interfaces 2015;7(8):4463–70.
[38] Chhetry A, Sharifuzzaman M, Yoon H, Sharma S, Xuan X, Park JY. MoS2-Decorated laser-induced graphene for a highly sensitive, hysteresis-free, and reliable piezoresistive strain sensor. ACS Appl Mater Interfaces 2019;11(25):22531–42.